

**DESY 12-235**  
**December 2012**

**ISSN 0418-9833**

Modern Physics Letters A  
 © World Scientific Publishing Company

**NEXT-TO-LEADING-ORDER TESTS OF NONRELATIVISTIC-QCD  
 FACTORIZATION WITH  $J/\psi$  YIELD AND POLARIZATION**

MATHIAS BUTENSCHOEN

*Universität Wien, Fakultät für Physik,  
 Boltzmannngasse 5, 1090 Wien, Austria  
 mathias.butenschoen@univie.ac.at*

BERND A. KNIEHL

*II. Institut für Theoretische Physik, Universität Hamburg,  
 Luruper Chaussee 149, 22761 Hamburg, Germany  
 kniehl@desy.de*

Received (Day Month Year)

Revised (Day Month Year)

We report on recent progress in testing the factorization formalism of nonrelativistic quantum chromodynamics (NRQCD) at next-to-leading order (NLO) for  $J/\psi$  yield and polarization. We demonstrate that it is possible to unambiguously determine the leading color-octet long-distance matrix elements (LDMEs) in compliance with the velocity scaling rules through a global fit to experimental data of unpolarized  $J/\psi$  production in  $pp$ ,  $p\bar{p}$ ,  $ep$ ,  $\gamma\gamma$ , and  $e^+e^-$  collisions. Three data sets not included in the fit, from hadroproduction and from photoproduction in the fixed-target and colliding-beam modes, are nicely reproduced. The polarization observables measured in different frames at DESY HERA and CERN LHC reasonably agree with NLO NRQCD predictions obtained using the LDMEs extracted from the global fit, while measurements at the FNAL Tevatron exhibit severe disagreement. We demonstrate that alternative LDME sets recently obtained, with different philosophies, in two other NLO NRQCD analyses of  $J/\psi$  yield and polarization also fail to reconcile the Tevatron polarization data with the other available world data.

*Keywords:*  $J/\psi$  meson; nonrelativistic QCD; factorization.

PACS Nos.: 12.38.Bx, 13.60.Le, 13.88.+e, 14.40.Pq

## 1. Introduction

While the overly successful experiments at the LHC are exploring the Higgs sector and are systematically searching for signals of physics beyond the standard model (SM), we must not be carried away losing track of a longstanding, unresolved puzzle in quantum chromodynamics (QCD), the otherwise well-established SU(3) gauge theory of the strong interactions, right in the core of the SM. In fact, despite concerted experimental and theoretical efforts ever since the discovery of the  $J/\psi$  meson in the November revolution of 1974 (The Nobel Prize in Physics 1976), the genuine mechanism underlying the production and decay of heavy quarkonia,

which are QCD bound states of a heavy quark  $Q = c, b$  and its antiparticle  $\bar{Q}$ , has remained mysterious.

Nonrelativistic QCD (NRQCD)<sup>1</sup> endowed with an appropriate factorization theorem, which was conjectured in a seminal work by Bodwin, Braaten, and Lepage<sup>2</sup> and explicitly proven through next-to-next-to-leading order for large transverse momenta  $p_T$ ,<sup>3,4</sup> arguably constitutes the most probable candidate theory at the present time. This implies a separation of process-dependent short-distance coefficients, to be calculated perturbatively as expansions in the strong-coupling constant  $\alpha_s$ , from supposedly universal long-distance matrix elements (LDMEs), to be extracted from experiment. The relative importance of the latter can be estimated by means of velocity scaling rules,<sup>5</sup> which predict each of the LDMEs to scale with a definite power of the heavy-quark velocity  $v$  in the limit  $v \ll 1$ . In this way, the theoretical predictions are organized as double expansions in  $\alpha_s$  and  $v$ . A crucial feature of this formalism is that the  $Q\bar{Q}$  pair can at short distances be produced in any Fock state  $n = {}^{2S+1}L_J^{[a]}$  with definite spin  $S$ , orbital angular momentum  $L$ , total angular momentum  $J$ , and color multiplicity  $a = 1, 8$ . In particular, this formalism predicts the existence of intermediate color-octet (CO) states in nature, which subsequently evolve into physical, color-singlet (CS) quarkonia by the nonperturbative emission of soft gluons. In the limit  $v \rightarrow 0$ , the traditional CS model (CSM) is recovered in the case of  $S$ -wave quarkonia. In the case of  $J/\psi$  production, the CSM prediction is based just on the  ${}^3S_1^{[1]}$  CS state, while the leading relativistic corrections, of relative order  $\mathcal{O}(v^4)$ , are built up by the  ${}^1S_0^{[8]}$ ,  ${}^3S_1^{[8]}$ , and  ${}^3P_J^{[8]}$  ( $J = 0, 1, 2$ ) CO states.

The CSM is not a complete theory, as may be understood by noticing that the next-to-leading-order (NLO) treatment of  $P$ -wave quarkonia is plagued by uncanceled infrared singularities, which are, however, properly removed in NRQCD. This conceptual problem cannot be cured from within the CSM, neither by proceeding to higher orders nor by invoking  $k_T$  factorization *etc.* In a way, NRQCD factorization,<sup>2</sup> appropriately improved at large values of  $p_T$  by systematic expansion in powers of  $m_Q^2/p_T^2$ ,<sup>6,7,8</sup> is the only game in town, which makes its experimental verification such a matter of paramount importance and general interest.<sup>9</sup>

The experimental test of NRQCD factorization<sup>2</sup> has been among the most urgent tasks on the agenda of the international quarkonium community<sup>9</sup> for almost two decades and, with high-quality data being so copiously harvested at the LHC, is now more tantalizing than ever. In the following, we discuss the present status of testing NRQCD factorization in charmonium production.

## 2. Global fit to measurements of unpolarized $J/\psi$ yields

We consider the inclusive production of  $J/\psi$  mesons in collisions of two particles  $A$  and  $B$ . Owing to the factorization theorems of the QCD parton model and

Table 1. NLO NRQCD fit results for the  $J/\psi$  CO LDMEs.<sup>18</sup> Subtracting from the data the estimated contributions from the feed-down of heavier charmonia, which are not included in the calculations, improves the quality of the fit.

|   | set A: unsubtracted                             | set B: subtracted                               |
|---|---|---|
| $\langle \mathcal{O}^{J/\psi}(^1S_0^{[8]}) \rangle$ | $(4.97 \pm 0.44) \times 10^{-2} \text{ GeV}^3$  | $(3.04 \pm 0.35) \times 10^{-2} \text{ GeV}^3$  |
| $\langle \mathcal{O}^{J/\psi}(^3S_1^{[8]}) \rangle$ | $(2.24 \pm 0.59) \times 10^{-3} \text{ GeV}^3$  | $(1.68 \pm 0.46) \times 10^{-3} \text{ GeV}^3$  |
| $\langle \mathcal{O}^{J/\psi}(^3P_0^{[8]}) \rangle$ | $(-1.61 \pm 0.20) \times 10^{-2} \text{ GeV}^5$ | $(-9.08 \pm 1.61) \times 10^{-3} \text{ GeV}^5$ |
| $\chi_{\text{d.o.f.}}^2$                            | 4.42  | 3.74  |

NRQCD,<sup>2</sup> the cross section is calculated as

$$d\sigma(AB \rightarrow J/\psi + X) = \sum_{i,j,k,l,n} \int dx_1 dx_2 dy_1 dy_2 f_{i/A}(x_1) f_{k/i}(y_1) f_{j/B}(x_2) f_{l/j}(y_2) \times \langle \mathcal{O}^{J/\psi}[n] \rangle d\sigma(kl \rightarrow c\bar{c}[n] + X), \quad (1)$$

where  $f_{i/A}(x_1)$  is the parton distribution function (PDF) of parton  $i = g, q, \bar{q}$  in hadron  $A = p, \bar{p}$  or the flux function of photon  $i = \gamma$  in charged lepton  $A = e^-, e^+$ ,  $f_{k/i}(y_1)$  is  $\delta_{ik}\delta(1-y_1)$  or the PDF of parton  $k$  in the resolved photon  $i$ ,  $d\sigma(kl \rightarrow c\bar{c}[n] + X)$  are the partonic cross sections, and  $\langle \mathcal{O}^{J/\psi}[n] \rangle$  are the LDMEs. In the fixed-flavor-number scheme, we have  $q = u, d, s$ . In the case of  $e^+e^-$  annihilation, all distribution functions in Eq. (1) are delta functions. The hadronic system  $X$  always contains one hard parton at leading order (LO) and is taken to be void of heavy flavors, which may be tagged and vetoed experimentally.<sup>10,11</sup> The partonic cross sections appropriate for the direct production of unpolarized  $J/\psi$  mesons were calculated at NLO in NRQCD in Refs. 12, 13 for direct photoproduction, in Refs. 14, 15, 16, 17 for hadroproduction, and in Ref. 18 for resolved photoproduction, two-photon scattering involving both direct and resolved photons, and  $e^+e^-$  annihilation.

In our numerical analysis, we set  $m_c = 1.5 \text{ GeV}$ , adopt the values of  $m_e, \alpha$ , and the branching ratios  $B(J/\psi \rightarrow e^+e^-)$  and  $B(J/\psi \rightarrow \mu^+\mu^-)$  from Ref. 19, and use the one-loop (two-loop) formula for  $\alpha_s^{(n_f)}(\mu)$ , with  $n_f = 4$  active quark flavors, at LO (NLO). As for the proton PDFs, we use set CTEQ6L1 (CTEQ6M)<sup>20</sup> at LO (NLO), which comes with an asymptotic scale parameter of  $\Lambda_{\text{QCD}}^{(4)} = 215 \text{ MeV}$  (326 MeV). As for the photon PDFs, we employ the best-fit set AFG04\_BF of Ref. 21. We evaluate the photon flux function using Eq. (5) of Ref. 22, with the upper cutoff on the photon virtuality  $Q^2$  chosen as in the considered data set. As for the CS LDME, we adopt the value  $\langle \mathcal{O}^{J/\psi}(^3S_1^{[1]}) \rangle = 1.32 \text{ GeV}^3$  from Ref. 23. Our default choices for the renormalization, factorization, and NRQCD scales are  $\mu_r = \mu_f = m_T$  and  $\mu_\Lambda = m_c$ , respectively, where  $m_T = \sqrt{p_T^2 + 4m_c^2}$  is the  $J/\psi$  transverse mass. The bulk of the theoretical uncertainty is due to the lack of knowledge of corrections beyond NLO, which are estimated by varying  $\mu_r, \mu_f$ , and  $\mu_\Lambda$  by a factor 2 up and down relative to their default values.

In Ref. 18, we performed a global fit to high-quality data of inclusive unpolarized  $J/\psi$  production, comprising a total of 194 data points from 26 data sets. Specifically, these included  $p_T$  distributions in hadroproduction from PHENIX<sup>24</sup> at RHIC, CDF at Tevatron I<sup>25,26</sup> and II,<sup>27</sup> ATLAS,<sup>28,29</sup> CMS,<sup>30</sup> ALICE,<sup>31</sup> and LHCb<sup>32</sup> at the LHC;  $p_T^2$ ,  $W$ , and  $z$  distributions in photoproduction from H1<sup>33</sup> and ZEUS<sup>34</sup> at HERA I and H1<sup>35</sup> at HERA II; a  $p_T^2$  distribution in two-photon scattering from DELPHI<sup>36</sup> at LEP II; and a total cross section in  $e^+e^-$  annihilation from Belle<sup>10</sup> at KEKB. Denoting the photon, proton, and  $J/\psi$  four-momenta by  $p_\gamma$ ,  $p_p$ , and  $p_{J/\psi}$ , respectively,  $W = \sqrt{(p_\gamma + p_p)^2}$  is the  $\gamma p$  center-of-mass energy and  $z = (p_{J/\psi} \cdot p_p)/(p_\gamma \cdot p_p)$  is the inelasticity variable measuring the fraction of the photon energy passed on to the  $J/\psi$  meson in the proton rest frame. We excluded from our fit all data points of two-photon scattering with  $p_T < 1$  GeV and of hadroproduction with  $p_T < 3$  GeV, which cannot be successfully described by our fixed-order calculations as expected. The fit results for the CO LDMEs obtained at NLO in NRQCD with default scale choices are collected in Table 1. They depend only feebly on the precise locations of the  $p_T$  cuts.

Our calculations refer to direct  $J/\psi$  production, as the data from Tevatron I<sup>25,26</sup> do, while the data from Tevatron II,<sup>27</sup> LHC,<sup>28,29,30,31,32</sup> and KEKB<sup>10</sup> comprise prompt events and those from RHIC,<sup>24</sup> HERA,<sup>33,34,35</sup> and LEP II<sup>36</sup> even non-prompt ones. The fit results obtained neglecting the effects due to these admixtures are listed in the second column of Table 1 (set A). However, the resulting error is small against our theoretical uncertainties and has no effect on our conclusions. In fact, the fraction of  $J/\psi$  events originating from the feed-down of heavier charmonia only amounts to about 36% for hadroproduction,<sup>25</sup> 15% for photoproduction at HERA,<sup>35</sup> 9% for two-photon scattering at LEP II,<sup>37</sup> and 26% for  $e^+e^-$  annihilation at KEKB,<sup>38</sup> and the fraction of  $J/\psi$  events from  $B$  decays is negligible RHIC, HERA,<sup>35</sup> and LEP II<sup>37</sup> energies. Refitting the data with the estimated feed-down contributions subtracted yields the values listed in the third column of Table 1 (set B). The  $\chi^2$  values per data point achieved by the two fits, which are specified as  $\chi_{\text{d.o.f.}}^2$  in Table 1, are to be taken with a grain of salt, since they do not take into account the theoretical uncertainties, which exceed most of the experimental errors.

The fact that the global fit<sup>18</sup> successfully pins down the three CO LDMEs as it does is quite nontrivial by itself and establishes their universality, the more so as the long-standing difficulty of NRQCD to describe the photoproduction data at large values of  $z$  is overcome. Furthermore, their values are of order  $\mathcal{O}(v^4)$  with respect to the CS LDME  $\langle \mathcal{O}^{J/\psi}(^3S_1^{[1]}) \rangle$ ,<sup>23</sup> in compliance with the velocity scaling rules.<sup>5</sup> Both observations consolidate the validity of NRQCD factorization as far as the unpolarized  $J/\psi$  yield is concerned.

In Fig. 1, all data sets fitted to are compared with our default NLO NRQCD results (solid lines). For comparison, also the default results at LO (dashed lines) as well as those of the CSM at NLO (dot-dashed lines) and LO (dotted lines) are shown. In order to visualize the size of the NLO corrections to the hard-scattering cross sections, the LO predictions are evaluated with the same LDMEs and PDFs.

The yellow and blue (shaded) bands indicate the theoretical errors on the NLO NRQCD and CSM results. We observe from Fig. 1 that the experimental data are nicely described by NLO NRQCD, being almost exclusively contained within its error bands, while they overshoot the NLO CSM predictions typically by 1–2 orders of magnitude for hadroproduction and a factor of 3–5 for photoproduction. In contrast to the LO analysis of Ref. 39, the DELPHI data<sup>36</sup> tend to systematically overshoot the NLO NRQCD result, albeit the deviation is by no means significant in view of the sizable experimental errors. This may be attributed to the destructive interference of the  $^1S_0^{[8]}$  and  $^3P_J^{[8]}$  contributions, which is a genuine NLO phenomenon. We have to bear in mind, however, that the DELPHI measurement comprises only 16 events with  $p_T > 1$  GeV and has not been confirmed by any of the other three LEP II experiments. The Belle measurement,  $\sigma(e^+e^- \rightarrow J/\psi + X) = (0.43 \pm 0.13)$  pb,<sup>10</sup> is compatible both with the NLO NRQCD and CSM results,  $(0.70^{+0.35}_{-0.17})$  pb and  $(0.24^{+0.20}_{-0.09})$  pb, respectively. However, the measured cross section was actually obtained from a data sample with the multiplicity of charged tracks in the events being larger than four, and corrections for the effect of this requirement were not performed, so that the value quoted in Ref. 10 just gives a lower bound on the cross section.

### 3. Further tests of NRQCD factorization in unpolarized $J/\psi$ production

Three data sets not included in the global fit,<sup>18</sup> from hadroproduction and from photoproduction in the fixed-target and colliding-beam modes, are nicely reproduced by our NLO NRQCD predictions, as may be seen from Figs. 2 and 3. They were taken by the ATLAS Collaboration<sup>40</sup> at the LHC, by Denby et al.<sup>41</sup> at the Fermilab Tagged-Photon Spectrometer, and by the ZEUS Collaboration<sup>42</sup> at HERA II. The  $\chi^2_{\text{d.o.f.}}$  values evaluated using our default NLO NRQCD predictions read 10.74,<sup>a</sup> 0.40, and 7.50, respectively. We conclude that NRQCD factorization passes this non-trivial test, which, in the case of Refs. 40, 41, probes kinematic regions far outside those covered by the global fit.<sup>18</sup>

### 4. $J/\psi$ polarization

The polarization of the  $J/\psi$  meson is conveniently analyzed experimentally by measuring the angular distribution of its leptonic decays, which is customarily parametrized using the three polarization observables  $\lambda_\theta$ ,  $\lambda_\phi$ , and  $\lambda_{\theta\phi}$ , as<sup>43</sup>

$$W(\theta, \phi) \propto 1 + \lambda_\theta \cos^2 \theta + \lambda_\phi \sin^2 \theta \cos(2\phi) + \lambda_{\theta\phi} \sin(2\theta) \cos \phi, \quad (2)$$

where  $\theta$  and  $\phi$  are respectively the polar and azimuthal angles of  $l^+$  in the  $J/\psi$  rest frame. This definition depends on the choice of coordinate frame. In the experimental analyses,<sup>35,44,45,46,47</sup> the helicity (recoil), Collins-Soper, and target

<sup>a</sup>This value is reduced to 4.88 if the data point at the largest value of  $p_T$  is omitted.

6 *Mathias Butenschoen, Bernd A. Kniehl*

frames were employed, in which the polar axes point in the directions of  $-(\vec{p}_p + \vec{p}_{\bar{p}})$ ,  $\vec{p}_p/|\vec{p}_p| - \vec{p}_{\bar{p}}/|\vec{p}_{\bar{p}}|$ , and  $-\vec{p}_p$ , respectively. The values  $\lambda_\theta = 0, +1, -1$  correspond to unpolarized, fully transversely polarized, and fully longitudinally polarized  $J/\psi$  mesons, respectively. The alternative notation  $\lambda = \lambda_\theta$ ,  $\mu = \lambda_{\theta\phi}$ , and  $\nu = 2\lambda_\phi$  is frequently encountered in the literature. In Refs. 45, 46,  $\lambda_\theta$  is called  $\alpha$ .

Working in the spin density matrix formalism and denoting the  $z$  component of  $S$  by  $i, j = 0, \pm 1$ , we have

$$\lambda_\theta = \frac{d\sigma_{11} - d\sigma_{00}}{d\sigma_{11} + d\sigma_{00}}, \quad \lambda_\phi = \frac{d\sigma_{1,-1}}{d\sigma_{11} + d\sigma_{00}}, \quad \lambda_{\theta\phi} = \frac{\sqrt{2} \operatorname{Re} d\sigma_{10}}{d\sigma_{11} + d\sigma_{00}}, \quad (3)$$

where  $d\sigma_{ij}$  is the  $ij$  component of the differential cross section. An expression of  $d\sigma_{ij}$  in terms of PDFs and partonic spin density matrix elements may be found in Eq. (3) of Ref. 48.

Our results for direct photoproduction<sup>48</sup> are shown in Fig. 4. We compare our NLO predictions for the parameters  $\lambda$  and  $\nu$  as functions of  $p_T$  and  $z$  with measurements by the H1 Collaboration<sup>35</sup> in the helicity and Collins-Soper frames and by the ZEUS Collaboration<sup>44</sup> in the target frame. Unfortunately, the H1<sup>35</sup> and ZEUS<sup>44</sup> data do not yet allow us to distinguish the production mechanisms clearly. However, kinematical regions can be identified in which a clear distinction could be possible in more precise experiments at a future  $ep$  collider, such as the CERN LHeC.<sup>49</sup> At higher values of  $p_T$ , NRQCD predicts the  $J/\psi$  meson to be largely unpolarized, in contrast to the CSM. In the  $z$  distributions, the scale uncertainties are sizable, and the error bands of the CSM and NRQCD predictions largely overlap.

Our results for direct hadroproduction<sup>50,51</sup> are shown in Fig. 5. We compare our predictions for the parameters  $\lambda_\theta$  and  $\lambda_\phi$  as functions of  $p_T$  in the helicity and Collins-Soper frames with the measurements by CDF<sup>45,46</sup> and ALICE.<sup>47</sup> In the helicity frame, the CSM predicts the  $J/\psi$  polarization to be strongly longitudinal at NLO, while NRQCD predicts it to be strongly transverse. In the Collins-Soper frame, the situation is inverted. The precise CDF measurement at Tevatron run II,<sup>46</sup> which is partially in disagreement with the one at run I,<sup>45</sup> found the  $J/\psi$  mesons to be largely unpolarized in the helicity frame, which is in contradiction with both the CSM and NRQCD predictions at NLO. The early ALICE data<sup>47</sup> is, however, compatible with NRQCD at NLO, favoring NRQCD over the CSM.

## 5. Comparisons with the literature

After our NLO NRQCD studies of  $J/\psi$  polarization,<sup>48,50,51</sup> two others appeared, which are, however, limited to hadroproduction. In Ref. 52, it was shown that the measured hadroproduction cross sections and the CDF II polarization measurement can be simultaneously described by NRQCD at NLO with one of the three CO LDME sets listed in the fourth column of Table 2. In Ref. 53, the polarization of promptly produced  $J/\psi$  mesons was studied by also including the feed-down from polarized  $\chi_{cJ}$  and  $\psi'$  mesons as described in Refs. 54, 55. To this end, the CO LDMEs of the  $\chi_{cJ}$  and  $\psi'$  mesons were fitted to LHCb (and CDF) unpolarized

production data, and the resulting cascade decay rates into  $J/\psi$  mesons were then used as feed-down contributions to determine the  $J/\psi$  CO LDMEs in a fit to unpolarized  $J/\psi$  production data from LHCb and CDF with  $p_T > 7$  GeV. The resulting LDMEs may be found in the third column of Table 2. Reference 53 predicts the  $J/\psi$  polarization to be moderately transverse in the helicity frame.

In Fig. 6, we systematically compare the analyses of Refs. 50, 51, 52, 53 as represented by the CO LDME sets in Table 2 with regard to their performances in describing the unpolarized  $J/\psi$  yields measured in  $e^+e^-$  annihilation by Belle,<sup>10</sup> in photoproduction by H1,<sup>33,35</sup> and in hadroproduction by CDF II<sup>27</sup> and ATLAS,<sup>40</sup> as well as the  $J/\psi$  polarization observable  $\lambda_\theta$  in the helicity frame as measured by CDF II.<sup>46</sup> We observe that none of the LDME sets can describe all the data sets. While the CO LDMEs of Ref. 18 yield a good description of the unpolarized  $J/\psi$  yields, there is a strong disagreement with the CDF II measurement of  $J/\psi$  polarization. On the other hand, the CO LDMEs of Ref. 52 can describe all hadroproduction data, but lead to overshoots by factors of 4–6 for  $e^+e^-$  annihilation and photoproduction. Finally, the CO LDMEs of Ref. 53 yield predictions which, in all cases, fall between those of the other two options.

Table 2. LDME sets determined in Refs. 18, 52, 53 and used in Fig. 6. In Ref. 52, two alternative sets are provided besides the default one. The analyses of Refs. 50, 51, 52 only refer to direct  $J/\psi$  production.

|   | Butenschoen,<br>Kniehl <sup>18</sup> | Gong, Wang,<br>Wan, Zhang <sup>53</sup> | Chao, Ma, Shao, Wang, Zhang <sup>52</sup><br>default set | set 2                  | set 3                 |
|---|--------------------------------------|---|--|------------------------|-----------------------|
| $\langle \mathcal{O}^{J/\psi}({}^3S_1^{[1]}) \rangle$ | 1.32 GeV <sup>3</sup>                | 1.16 GeV <sup>3</sup>                   | 1.16 GeV <sup>3</sup>                                    | 1.16 GeV <sup>3</sup>  | 1.16 GeV <sup>3</sup> |
| $\langle \mathcal{O}^{J/\psi}({}^1S_0^{[8]}) \rangle$ | 0.0497 GeV <sup>3</sup>              | 0.097 GeV <sup>3</sup>                  | 0.089 GeV <sup>3</sup>                                   | 0                      | 0.11 GeV <sup>3</sup> |
| $\langle \mathcal{O}^{J/\psi}({}^3S_1^{[8]}) \rangle$ | 0.0022 GeV <sup>3</sup>              | -0.0046 GeV <sup>3</sup>                | 0.0030 GeV <sup>3</sup>                                  | 0.014 GeV <sup>3</sup> | 0                     |
| $\langle \mathcal{O}^{J/\psi}({}^3P_0^{[8]}) \rangle$ | -0.0161 GeV <sup>5</sup>             | -0.0214 GeV <sup>5</sup>                | 0.0126 GeV <sup>5</sup>                                  | 0.054 GeV <sup>5</sup> | 0                     |
| $\langle \mathcal{O}^{\psi'}({}^3S_1^{[1]}) \rangle$  |                                      | 0.758 GeV <sup>3</sup>                  |  |                        |                       |
| $\langle \mathcal{O}^{\psi'}({}^1S_0^{[8]}) \rangle$  |                                      | -0.0001 GeV <sup>3</sup>                |  |                        |                       |
| $\langle \mathcal{O}^{\psi'}({}^3S_1^{[8]}) \rangle$  |                                      | 0.0034 GeV <sup>3</sup>                 |  |                        |                       |
| $\langle \mathcal{O}^{\psi'}({}^3P_0^{[8]}) \rangle$  |                                      | 0.0095 GeV <sup>5</sup>                 |  |                        |                       |
| $\langle \mathcal{O}^{\chi_0}({}^3P_0^{[1]}) \rangle$ |                                      | 0.107 GeV <sup>5</sup>                  |  |                        |                       |
| $\langle \mathcal{O}^{\chi_0}({}^3S_1^{[8]}) \rangle$ |                                      | 0.0022 GeV <sup>3</sup>                 |  |                        |                       |

## 6. Conclusions

As for the unpolarized  $J/\psi$  yield, NRQCD factorization was consolidated at NLO by a global fit to the world's data of hadroproduction, photoproduction, two-photon scattering, and  $e^+e^-$  annihilation,<sup>18</sup> which successfully pinned down the three CO LDMEs in compliance with the velocity scaling rules and impressively supported their universality. In a second step, NLO NRQCD predictions of  $J/\psi$  polarization observables in various reference frames were confronted with measurements

in photoproduction at HERA and hadroproduction at the Tevatron and the LHC. In the case of hadroproduction at the Tevatron, the prediction of strongly transverse  $J/\psi$  polarization in the helicity frame stands in severe contrast to the precise CDF II measurement,<sup>46</sup> which found the  $J/\psi$  mesons to be unpolarized. Using the CO LDME sets recently extracted from hadroproduction data by two other groups<sup>52,53</sup> does not help us to reach a satisfactory description of all the available precision data. Thus, we conclude that the universality of the  $J/\psi$  production LDMEs is challenged. Possible remedies include the following:

- (i) The eagerly awaited  $J/\psi$  polarization measurements at the LHC might not confirm the CDF II results.
- (ii) Although unlikely, measurements at a future  $ep$  collider, such as the LHeC,<sup>49</sup> might reveal that the  $p_T$  distribution of  $J/\psi$  photoproduction exhibits a drastically weaker slope beyond  $p_T = 10$  GeV, the reach of HERA, so that the LDME sets of Refs. 52, 53 might yield better agreement with the data there.
- (iii) The assumption that the  $v$  expansion is convergent might not be valid for charmonium, leaving the possibility that the LDME universality is intact.

### Acknowledgment

This work was supported in part by the German Federal Ministry for Education and Research BMBF through Grant No. 05H12GUE and by the Helmholtz Association HGF through Grant No. Ha 101.

### References

1. W. E. Caswell and G. P. Lepage, *Phys. Lett. B* **167**, 437 (1986).
2. G. T. Bodwin, E. Braaten, and G. P. Lepage, *Phys. Rev. D* **51**, 1125 (1995); **55**, 5853(E) (1997) [hep-ph/9407339].
3. G. C. Nayak, J.-W. Qiu, and G. F. Sterman, *Phys. Rev. D* **72**, 114012 (2005) [hep-ph/0509021].
4. G. C. Nayak, J. W. Qiu, and G. F. Sterman, *Phys. Rev. D* **74**, 074007 (2006) [hep-ph/0608066].
5. G. P. Lepage, L. Magnea, C. Nakhleh, U. Magnea, and K. Hornbostel, *Phys. Rev. D* **46**, 4052 (1992) [hep-lat/9205007].
6. Z.-B. Kang, J.-W. Qiu, and G. Sterman, *Nucl. Phys. B (Proc. Suppl.)* **214**, 39 (2011).
7. Z.-B. Kang, J.-W. Qiu, and G. Sterman, *Phys. Rev. Lett.* **108**, 102002 (2012) [arXiv:1109.1520 [hep-ph]].
8. S. Fleming, A. K. Leibovich, T. Mehen, and I. Z. Rothstein, *Phys. Rev. D* **86**, 094012 (2012) [arXiv:1207.2578 [hep-ph]].
9. N. Brambilla *et al.* (Quarkonium Working Group), *Eur. Phys. J. C* **71**, 1534 (2011) [arXiv:1010.5827 [hep-ph]].
10. P. Pakhlov *et al.* (Belle Collaboration), *Phys. Rev. D* **79**, 071101 (2009) [arXiv:0901.2775 [hep-ex]].
11. R. Aaij *et al.* (LHCb Collaboration), *JHEP* **1206**, 141 (2012) [arXiv:1205.0975 [hep-ex]].
12. M. Butenschön and B. A. Kniehl, *Phys. Rev. Lett.* **104**, 072001 (2010) [arXiv:0909.2798 [hep-ph]].



13. M. Butenschön and B. A. Kniehl, PoS(DIS 2010)157 [arXiv:1006.1776 [hep-ph]].
14. M. Butenschön and B. A. Kniehl, *Phys. Rev. Lett.* **106**, 022003 (2011) [arXiv:1009.5662 [hep-ph]].
15. M. Butenschoen and B. A. Kniehl, *AIP Conf. Proc.* **1343**, 409 (2011) [arXiv:1011.5619 [hep-ph]].
16. Y.-Q. Ma, K. Wang, and K.-T. Chao, *Phys. Rev. Lett.* **106**, 042002 (2011) [arXiv:1009.3655 [hep-ph]].
17. Y. Q. Ma, K. Wang, and K. T. Chao, *Phys. Rev. D* **84**, 114001 (2011) [arXiv:1012.1030 [hep-ph]].
18. M. Butenschoen and B. A. Kniehl, *Phys. Rev. D* **84**, R051501 (2011) [arXiv:1105.0820 [hep-ph]].
19. K. Nakamura *et al.* (Particle Data Group Collaboration), *J. Phys. G* **37**, 075021 (2010).
20. J. Pumplin, D. R. Stump, J. Huston, H.-L. Lai, P. Nadolsky, and W.-K. Tung (CTEQ Collaboration), *JHEP* **0207**, 012 (2002) [hep-ph/0201195].
21. P. Aurenche, M. Fontannaz, and J. Ph. Guillet, *Eur. Phys. J. C* **44**, 395 (2005) [hep-ph/0503259].
22. B. A. Kniehl, G. Kramer, and M. Spira, *Z. Phys. C* **76**, 689 (1997) [hep-ph/9610267].
23. G. T. Bodwin, H. S. Chung, D. Kang, J. Lee, and C. Yu, *Phys. Rev. D* **77**, 094017 (2008) [arXiv:0710.0994 [hep-ph]].
24. A. Adare *et al.* (PHENIX Collaboration), *Phys. Rev. D* **82**, 012001 (2010) [arXiv:0912.2082 [hep-ex]].
25. F. Abe *et al.* (CDF Collaboration), *Phys. Rev. Lett.* **79**, 572 (1997).
26. F. Abe *et al.* (CDF Collaboration), *Phys. Rev. Lett.* **79**, 578 (1997).
27. D. Acosta *et al.* (CDF Collaboration), *Phys. Rev. D* **71**, 032001 (2005) [hep-ex/0412071].
28. G. Aad *et al.* (ATLAS Collaboration), ATLAS Note ATLAS-CONF-2010-062.
29. J. Kirk (ATLAS Collaboration), PoS(ICHEP 2010)013.
30. V. Khachatryan *et al.* (CMS Collaboration), *Eur. Phys. J. C* **71**, 1575 (2011) [arXiv:1011.4193 [hep-ex]].
31. E. Scomparin (ALICE Collaboration), *Nucl. Phys. B (Proc. Suppl.)* **214**, 56 (2011).
32. R. Aaij *et al.* (LHCb Collaboration), *Eur. Phys. J. C* **71**, 1645 (2011) [arXiv:1103.0423 [hep-ex]].
33. C. Adloff *et al.* (H1 Collaboration), *Eur. Phys. J. C* **25**, 25 (2002) [arXiv:hep-ex/0205064].
34. S. Chekanov *et al.* (ZEUS Collaboration), *Eur. Phys. J. C* **27**, 173 (2003) [hep-ex/0211011].
35. F. D. Aaron *et al.* (H1 Collaboration), *Eur. Phys. J. C* **68**, 401 (2010) [arXiv:1002.0234 [hep-ex]].
36. J. Abdallah *et al.* (DELPHI Collaboration), *Phys. Lett. B* **565**, 76 (2003) [hep-ex/0307049].
37. M. Klasen, B. A. Kniehl, L. N. Mihaila, and M. Steinhauser, *Nucl. Phys. B* **713**, 487 (2005) [hep-ph/0407014].
38. Y.-Q. Ma, Y.-J. Zhang, and K.-T. Chao, *Phys. Rev. Lett.* **102**, 162002 (2009) [arXiv:0812.5106 [hep-ph]].
39. M. Klasen, B. A. Kniehl, L. N. Mihaila, and M. Steinhauser, *Phys. Rev. Lett.* **89**, 032001 (2002) [hep-ph/0112259].
40. G. Aad *et al.* (ATLAS Collaboration), *Nucl. Phys. B* **850**, 387 (2011) [arXiv:1104.3038 [hep-ex]].
41. B. H. Denby *et al.*, *Phys. Rev. Lett.* **52**, 795 (1984).

10 *Mathias Butenschoen, Bernd A. Kniehl*

42. H. Abramowicz *et al.* (ZEUS Collaboration), Report No. DESY 12-226 [arXiv:1211.6946 [hep-ex]].
43. C. S. Lam and W.-K. Tung, *Phys. Rev. D* **18**, 2447 (1978).
44. S. Chekanov *et al.* (ZEUS Collaboration), *JHEP* **0912**, 007 (2009) [arXiv:0906.1424 [hep-ex]].
45. T. Affolder *et al.* (CDF Collaboration), *Phys. Rev. Lett.* **85**, 2886 (2000) [arXiv:hep-ex/0004027].
46. A. Abulencia *et al.* (CDF Collaboration), *Phys. Rev. Lett.* **99**, 132001 (2007) [arXiv:0704.0638 [hep-ex]].
47. B. Abelev *et al.* (ALICE Collaboration), *Phys. Rev. Lett.* **108**, 082001 (2012) [arXiv:1111.1630 [hep-ex]].
48. M. Butenschoen and B. A. Kniehl, *Phys. Rev. Lett.* **107**, 232001 (2011) [arXiv:1109.1476 [hep-ph]].
49. N. Armesto (LHeC Study Group), *Frascati Phys. Ser.* **54**, 22 (2012).
50. M. Butenschoen and B. A. Kniehl, *Phys. Rev. Lett.* **108**, 172002 (2012) [arXiv:1201.1872 [hep-ph]].
51. M. Butenschoen and B. A. Kniehl, *Nucl. Phys. B (Proc. Suppl.)* **222–224**, 151 (2012) [arXiv:1201.3862 [hep-ph]].
52. K.-T. Chao, Y.-Q. Ma, H.-S. Shao, K. Wang, and Y.-J. Zhang, *Phys. Rev. Lett.* **108**, 242004 (2012) [arXiv:1201.2675 [hep-ph]].
53. B. Gong, L.-P. Wan, J.-X. Wang, and H.-F. Zhang, *Phys. Rev. Lett.* **110**, 042002 (2013) [arXiv:1205.6682 [hep-ph]].
54. E. Braaten, B. A. Kniehl, and J. Lee, *Phys. Rev. D* **62**, 094005 (2000) [hep-ph/9911436].
55. B. A. Kniehl and J. Lee, *Phys. Rev. D* **62**, 114027 (2000) [hep-ph/0007292].

Next-to-leading-order tests of nonrelativistic-QCD factorization with  $J/\psi$  yield and polarization 11

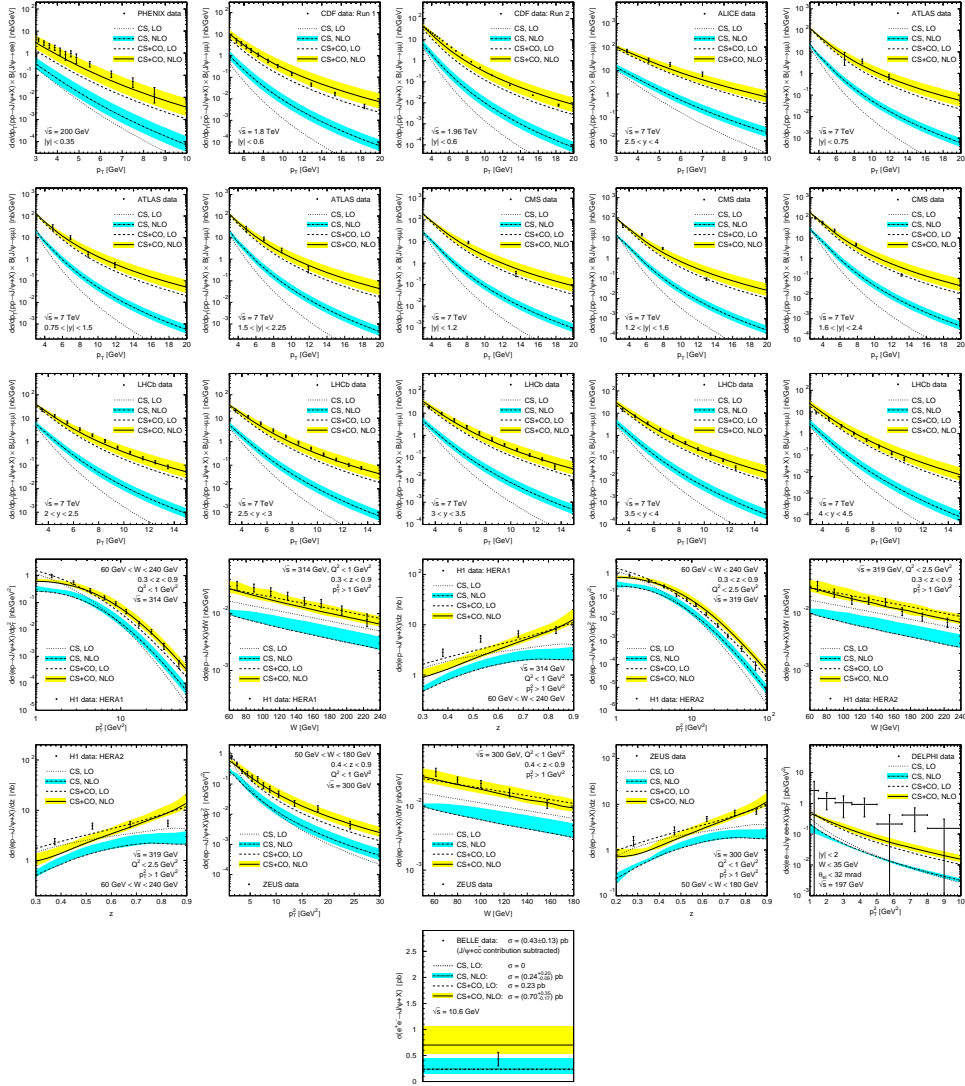


Fig. 1. NLO NRQCD fit<sup>18</sup> compared to RHIC,<sup>24</sup> Tevatron,<sup>25,26,27</sup> LHC,<sup>28,29,30,31,32</sup> HERA,<sup>33,34,35</sup> LEP II,<sup>36</sup> and KEKB<sup>10</sup> data.

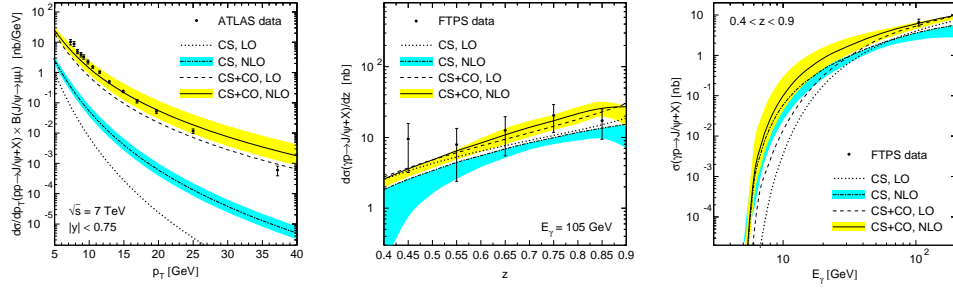
12 *Mathias Butenschoen, Bernd A. Kniehl*


Fig. 2. ATLAS data on  $J/\psi$  inclusive hadroproduction<sup>40</sup> and FTPS data on  $J/\psi$  inclusive photoproduction in the fixed-target mode<sup>41</sup> compared to NLO NRQCD predictions evaluated using set A of CO LDMEs from Table 1.

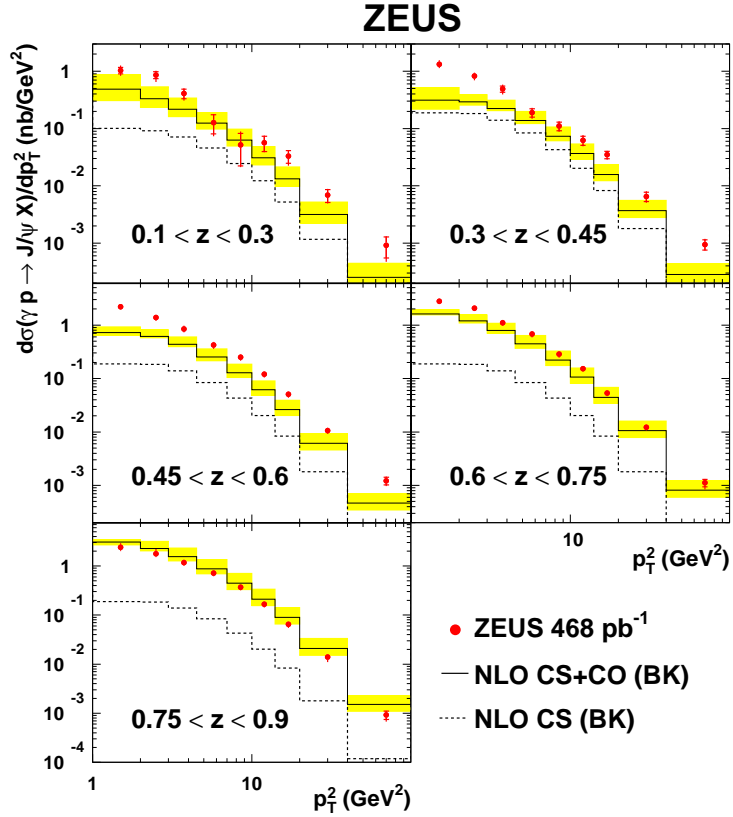


Fig. 3. ZEUS data on  $J/\psi$  inclusive photoproduction<sup>42</sup> compared to NLO NRQCD predictions evaluated using set A of CO LDMEs from Table 1.

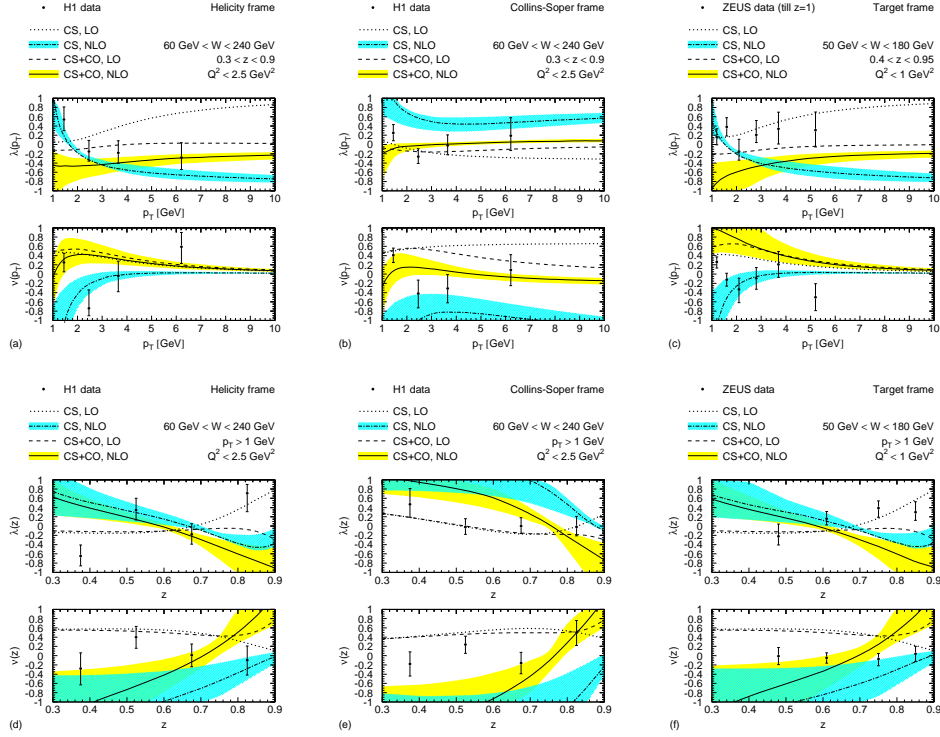


Fig. 4. The polarization parameters  $\lambda$  and  $\nu$  for direct photoproduction at HERA evaluated at NLO in the CSM and in NRQCD<sup>48</sup> using set B of CO LDME from Table 1 are compared to H1<sup>35</sup> and ZEUS<sup>44</sup> data. The theoretical uncertainties are due to scale variations in the CSM (blue bands) and include also the errors on the CO LDMEs (yellow bands) in NRQCD.

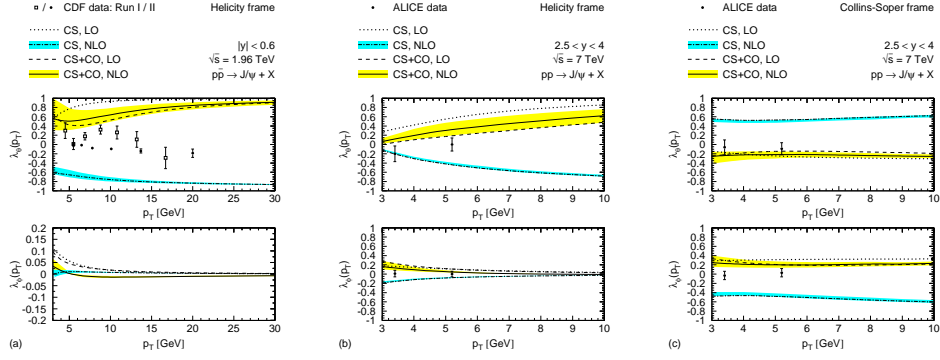
14 *Mathias Butenschoen, Bernd A. Kniehl*


Fig. 5. The polarization parameters  $\lambda_\theta$  and  $\lambda_\phi$  for hadroproduction evaluated at NLO in the CSM and in NRQCD<sup>50,51</sup> using set B of CO LDME from Table 1 are compared to CDF data from Tevatron runs I<sup>45</sup> and II<sup>46</sup> and to ALICE data.<sup>47</sup> The theoretical uncertainties are due to scale variations in the CSM (blue bands) and include also the errors on the CO LDMEs (yellow bands) in NRQCD.

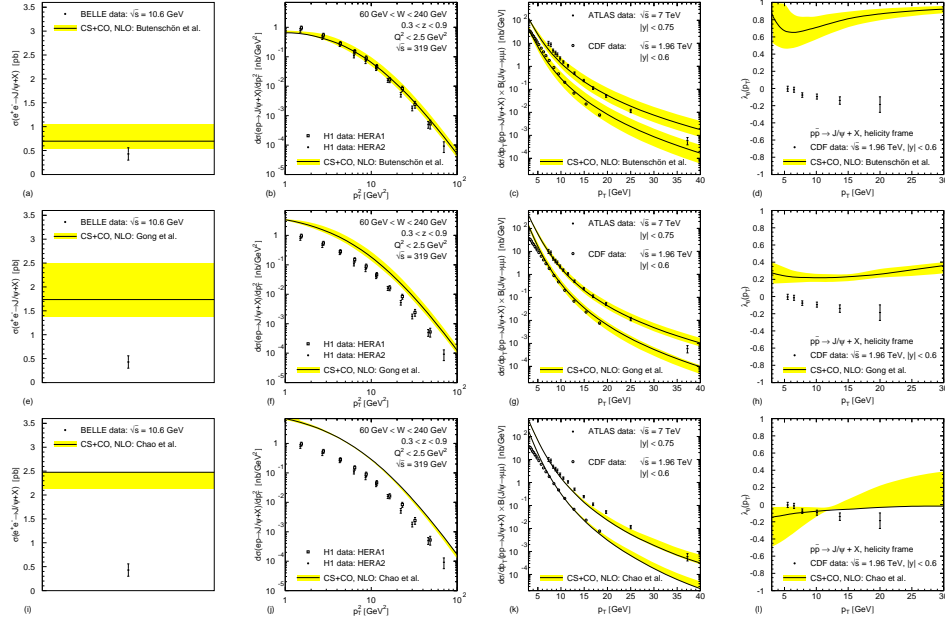


Fig. 6. The unpolarized  $J/\psi$  yields measured in  $e^+e^-$  annihilation by Belle,<sup>10</sup> in photoproduction by H1,<sup>33,35</sup> and in hadroproduction by CDF II<sup>27</sup> and ATLAS<sup>40</sup> as well as the  $J/\psi$  polarization observable  $\lambda_\theta$  in the helicity frame as measured by CDF II<sup>46</sup> are compared with the NLO NRQCD predictions evaluated using the CO LDME sets of Refs. 18, 52, 53 listed in Table 2. The theoretical errors in graphs a–g refer to scale variations, and those in graph d are obtained by also adding in quadrature the fit errors on the CO LDMEs according to Table 1. Graph h is taken over from Fig. 4 of Ref. 53. In graphs i–l, the central lines refer to the default CO LDME set of Ref. 52, and the theoretical errors are evaluated using the alternative CO LDME sets of Ref. 52.